Available online at www.sciencedirect.com
SCIENCE DIRECT
Journal of Catalysis 232 (2005) 210–225
JOURNAL OF CATALYSIS
www.elsevier.com/locate/jcat

Immobilization of molecular $H_3PW_{12}O_{40}$ heteropolyacid catalyst in alumina-grafted silica-gel and mesostructured SBA-15 silica matrices

P. Madhusudhan Rao [a], A. Wolfson [b], S. Kababya [c], S. Vega [c], M.V. Landau [a,*]

[a] *Chemical Engineering Department, Blechner Center of Applied Catalysis and Process Development, Ben-Gurion University of the Negev, Beer-Sheva 84105, Israel*

[b] *Chemical Engineering Department, Sami Shamoon College of Engineering Beer-Sheva, 84100, Israel*

[c] *Department of Chemical Physics, Weizmann Institute of Science, Rehovot 76100, Israel*

Received 30 December 2004; revised 2 March 2005; accepted 4 March 2005

Available online 12 April 2005

Abstract

The effects of grafting the alumina species at the surface of silica support on the $H_3PW_{12}O_{40}$ (HPW) immobilization capacity and performance of loaded HPW in acid-catalyzed reactions were studied with regular silica-gel and ordered mesostructured silica SBA-15. The states of alumina and HPW, in terms of the acidity/basicity, material texture, and structure of adsorbed HPW species, were characterized by XRD, XPS, NH_3-TPD, UV–vis-, and FTIR-spectroscopy, as well as ^1H and ^{31}P MAS NMR, NH_3- and CO_2-TPD, and N_2 adsorption. It was demonstrated that grafting of silica with small alumina clusters at partial to full surface coverage produces isolated basic sites of the same strength as at the surface of pure alumina, but with a surface concentration that is an order of magnitude lower. These sites anchor the molecular species of HPW, retaining their polyanion structure and acidity-catalytic activity patterns in several acid-catalyzed reactions. The reason for the low activity of HPW moieties immobilized at the surface of pure alumina is a polydentate adsorption of polyanions yielding a high extent of HPW acidity neutralization. The use of mesostructured SBA-15 as a support yielded catalysts with 30–70% higher activity compared with that based on regular silica gel. This is a result of higher surface area and surface concentration of silanols in SBA-15, which makes it possible to immobilize more HPW as molecular species.

Keywords: $H_3PW_{12}O_{40}$ heteropolyacid; Alumina-grafted silica-gel; Alumina-grafted SBA-15; ^{31}P MAS NMR; Acidity; Basicity; Acidic catalysis

1. Introduction

Environmental considerations and handling difficulties have led to sustained efforts in recent years to replace homogeneous acid catalysts, both Brønsted and Lewis types, with solid acid catalysts. Heteropolyacids, particularly the Keggin-type 12-tungstophosphoric acid (hereafter HPW), exhibit high acidic strengths and have performed admirably in a wide variety of acid-catalyzed reactions [1,2]. However, HPW suffers from drawbacks, such as very low surface area ($< 5\ m^2/g$), which hinders accessibility to the strong acidic sites, whereas high affinity for polar media renders it soluble. Attempts to overcome these drawbacks include partial neutralization of protons in HPW by different cations, resulting in the corresponding salts [2,3], embedding of HPW in supports by direct synthesis [4,5], and support of HPW on high surface area oxides [6–12]. Exchanging part of the protons of HPW with cations with higher ionic radii, like Cs^+ and NH_4^+, for example, allowed its separation and recycling. However, the high extent of ion exchange of alkali cations ($> 80\%$ of Cs) that was required to obtain full heterogenization of HPW resulted in significant lowering of catalyst acidity. This is compensated by an increase in the accessibility to the remaining acid sites due to formation of a solid possessing both micropores and mesopores [13,14]. Yet these salts tend to form colloidal suspensions in polar media, resulting in difficulties in the catalyst separation [13]. On the

* Corresponding author. Fax: +972 8 6477 678.
E-mail address: mlandau@bgumail.bgu.ac.il (M.V. Landau).

0021-9517/$ – see front matter
doi:10.1016/j.jcat.2005.03.006

other hand, embedded systems that involve the addition of HPW to the mixture for silica-gel synthesis resulted in its rigid binding in the host matrix, thereby mitigating leaching [15]. However, the high calcination temperature (723 K) employed for the formation of matrix pore structure in this case caused structural damage to the Keggin anions [15].

Several supports, such as silica gel [7,12], alumina [7–9], zirconia [15,16], carbon [7,17], and mesoporous silica [5,10,18], have been used to enhance the dispersion of HPW, thereby increasing the accessibility to their acid sites while lowering their solubility in polar media. Silica has been widely favored as the supporting material for HPW, since it interacts weakly with the Keggin anions and thus preserves their structure [7,10]. Yet in reactions that involve polar media, true heterogenization of HPW could not be achieved on silica, and the acid leached out into the reaction mixture [4,10,12,19]. On the other hand, the strong interaction of HPW with the metal-oxide support (e.g., in the case of alumina) results in a decline of its acidity [20]. These strong interactions were attributed to the high basicity of the support, which was derived from electronegativity calculations for various oxides [8] or by *n*-butylamine thermometric titration [8] and TPD of ammonia [21] for supported HPW catalysts. The detrimental effect of such interactions on catalytic activity has also been well documented [7–9].

To summarize, it is difficult to immobilize HPW on weakly interacting supports like silica, especially when polar reactants are used, whereas on strongly interacting supports like alumina, HPW loses its acidity. Therefore we can expect that a support with controlled strength and concentration of surface basic sites can prevent HPW leaching without destroying its acidity. Alumina is an amphotheric material with an average surface basicity formed by the dehydroxylation of its surface: (Al(OH)–O–Al(OH) $\rightarrow$ $Al^{(+)}$–O–Al–$O^{(-)}$ + H_2O [22,23]. Grafting of alumina species to the silica surface can weaken the detrimental interaction between HPW and alumina by diminishing the surface concentration of basic sites and/or decreasing their basic strength. This could provide an appropriate surface basicity to anchor HPW without losing its acidity. Based on this premise, we have recently reported the successful immobilization of HPW on alumina-grafted silica gel support, containing 2 and 8 wt% alumina with corresponding HPW loadings of 5 and 19 wt%, respectively [24]. Indeed, the HPW supported on alumina-grafted silica gel resisted leaching, unlike in silica-supported HPW catalysts. Catalytic activities comparable to those of pure acid, which acted homogeneously, were obtained after immobilization of HPW on alumina-grafted silica gel materials in the dehydration of isopropanol and MTBE synthesis from *t*-butanol and methanol. These activities were suppressed when the reactions were performed on pure alumina-supported HPW.

It has been reported previously that a loading of ~ 9 wt% alumina on silica gel by grafting yields full coverage, and multistep grafting results in bulk alumina behavior [25]. Alumina grafted to the ordered mesostructured silica (OMS) MCM-41 forms mostly small alumina clusters on its surface at low loadings and exhibits bulk-like behavior at a loading of 38 wt% [26,27]. It could be expected that employing OMS, with a higher capacity for grafted alumina species than on regular silica gel, can immobilize much more HPW and thereby improve the catalysts performance.

In the present study we investigated the effects of alumina grafting at the surface of silica gel and OMS of the SBA-15 type on the HPW immobilization capacity and performance of loaded HPW in acid-catalyzed reactions. The states of alumina and HPW, in terms of the acidity/basicity, material texture, and structure of adsorbed HPW species, were characterized by XRD, XPS, UV–vis-, and FTIR-spectroscopy, as well as ^1H and ^{31}P MAS NMR, NH_3- and CO_2-TPD, and N_2 adsorption. On the basis of characterization results we proposed a model of HPW adsorption on alumina-grafted silica supports that prevents its leaching in polar media and retains surface acidity and catalytic activity.

2. Experimental

2.1. Preparation of the catalysts

Commercial silica-gel (hereafter SG) (PQ Corp.; material 2287, powder fraction 40–60 mesh) and alumina (Norton Corp.; material 6176, crushed pellets with a 40–60 mesh fraction, a surface area of 250 m^2/g, and a pore volume of 0.95 cm^3/g) were used as supports. SBA-15 was prepared according to the procedure presented in [28] by crystallization from acidic, aqueous solutions of poly(ethylene glycol)–*block*-poly(propylene glycol)–*block*-poly(ethylene glycol) copolymer (Aldrich; $M_{avg.} = 5800$) and TMOS (Aldrich).

Alumina-grafted SG (AGSG) and alumina-grafted SBA-15 (AGSBA) supports were prepared by the treatment of SG or SBA-15 with a Al(O–*sec*-Bu)$_3$ (Aldrich) solution in anhydrous toluene (Aldrich) in the presence of triethylamine (Riedel–de-Haen) followed by hydrolysis and calcination at 773 K, according to a procedure described elsewhere [26]. The alumina content in the grafted silica-gel samples was controlled with the use of a Al(O–*sec*-Bu)$_3$ concentration of 5 and 50 g/l in toluene at the grafting stage. The alumina concentrations in AGSG after calcination were 2.1 wt% (AGSG-2) and 8.3 wt% (AGSG-8), respectively. In the second case the alumina content corresponds to the full adsorption capacity of silica gel. Repetition of the grafting procedure (with a 50 g/l solution) on AGSG-8 yielded a 16.1 wt% alumina-grafted AGSG (AGSG-16). Treatment of SBA-15 with Al(O–*sec*-Bu)$_3$-toluene solutions of 70 and 120 g/l yielded AGSBA samples with 8.6 wt% (AGSBA-9) and 16.9 wt% (AGSBA-17) grafted alumina, respectively. Repetition of the grafting procedure on AGSBA-17 (with a 120 g/l solution) yielded AGSBA-27 (with 27.4 wt% Al_2O_3) and, after an additional grafting step, AGSBA-38 (with 37.8 wt% Al_2O_3).

We inserted HPW by stirring 1 g of the support (SG, Al_2O_3, AGSG, or AGSBA) in a 10-ml methanolic solution containing 0.5 mmol of $H_3PW_{12}O_{40} \cdot 6H_2O$ (Aldrich) for 3 h at 298 K. The solid material was separated by filtration, washed with 250 cm^3 methanol, and dried overnight at 373 K.

2.2. Characterization methods

The HPW loading and the alumina content of the grafted silica samples were measured by energy-dispersive X-ray spectroscopy (EDS) with a JEOL JEM 5600 scanning electron microscope.

The surface area of the supports and the HPW catalysts and their pore size distributions were derived from nitrogen adsorption isotherms measured with a NOVA-2000 (Quantachrome, Version 7.02) instrument, with the use of BET and BJH methods, respectively. The samples were pretreated at 373 K under vacuum.

The small-angle X-ray scattering patterns of pure SBA-15- and SBA-15-based materials were measured as described in [26]. The conventional wide-angle XRD patterns were obtained on a Guinier G 670 camera (Cu-K_{α_1} radiation) connected to a rotating-anode X-ray source that was operated at 40 kV and 100 mA. The data were collected in the range of $2\theta = 3°$–$70°$ with a step size of 0.005°. The exposition time was 30 min, and the average size of the crystal domains was determined with Scherrer's equation, $h = K\lambda/[(B^2 - \beta^2)^{0.5}\cos(2\theta/2)]$, where $K = 1.000$ is the shape factor, $\lambda = 0.154$ nm, and β is the instrumental broadening correction. We determined the peak positions and the instrumental peak broadening by fitting each diffraction peak by means of APD computer software.

UV–visible spectra were recorded in the wavelength range of 200–300 nm on a V-560 spectrometer (JASCO Corp.) with a sensitivity that made it possible to detect 2 ppm of HPW. The infrared spectra of the supports and catalysts were recorded with a Nicolet Impact 460 spectrometer, with the use of KBr pellets (0.005 g sample and 0.1 g KBr), with 32 sample scans and a resolution of 1 cm^{-1}. The data were treated with OMNIC software. X-ray photoelectron spectra were acquired with a PHI 549 SAM/AES/XPS ultra-high-vacuum (10^{-9} Torr) apparatus with a double-cylindrical mirror analyzer (CMA) and a Mg-K_α (1253.6 eV) X-ray source. Powder samples of the catalysts were pressed on the indium-plated grid to a thin layer. We found the spectral component of the O signal by fitting a sum of single-component lines to the experimental data by means of nonlinear least-squares curve-fitting. The single-component lines were assumed to have the shape of a sum of a Cauchy and a Gaussian line shape, and the deconvolution was done according to [29]. The peak positions were calibrated relative to the carbon 1s peak positioned at 284.6 eV.

^{31}P and ^{1}H room-temperature NMR experiments were performed on a 300-MHz spectrometer at frequencies of 121.49 and 300.13 MHz, respectively. A BL 4-mm Bruker MAS probe was employed. The ^{31}P MAS NMR spectra were measured with the use of a single $\pi/2$ pulse, with a pulse duration of 5 μs and a repetition time of 10 s. High-power proton decoupling was employed with the TPPM scheme at a spinning speed of 5 kHz. Up to 6000 transients were accumulated, and the chemical shift scale was referenced to H_3PO_4 (85%). ^{1}H MAS NMR spectra were recorded with a Hahn echo sequence (τ 100 μs) with a pulse length of 5, 10 μs, a repetition time of 0.5 ms, and at a spinning frequency of 10 kHz. Four transients were accumulated, and the ^{1}H chemical shift scale was referenced to TMS. The samples were heated in air at 473 K for 2 h before their loading in the zirconium rotors.

Temperature-programmed desorption (TPD) of CO_2 was carried out on samples not containing HPW, with the use of an AMI-100 Catalyst Characterization System (Zeton–Altamira) equipped with a TCD detector and a mass spectrometer for identification of the outlet components (Ametek 1000). Approximately 0.35 g of sample was weighed and loaded into the reaction cell, heated in a helium atmosphere to 600 °C, and then cooled to 25 °C. A gaseous mixture, consisting of 5 vol% CO_2 in He, was passed over the sample at a rate of 25 cm^3/min for 1 h, followed by flushing with He for 0.5 h. Then the temperature was increased from ambient temperature to 600 °C at 10 °C/min^{-1} in a flow of helium, and the desorbed CO_2 was analyzed quantitatively.

TPD experiments with ammonia were performed on the supported HPW catalysts with the same setup. Approximately 0.4 g of catalyst was loaded into the sample holder, heated to 200 °C in argon, and subsequently cooled to 25 °C. After dosing with a 5 vol% ammonia:argon mixture for 30 min, the system was purged with argon for 1 h at the same temperature. The temperature was increased to 600 °C at a rate of 10 °C/min in a flow of argon, and the outlet gases were analyzed by mass spectrometry.

2.3. Testing of the catalysts

The immobilized HPW catalysts and the pure HPW acid were tested in three acid-catalyzed reactions: isopropanol (IP) dehydration, MTBE synthesis by condensation of *t*-butanol with methanol, and *tert*-butylation of catechol (Fig. 1). All of the HPW-containing catalysts were exposed for 2 h at 473 K to a nitrogen flow before the catalytic tests. The supports, alumina-grafted silicas and pure alumina, were activated at 773 K for 2 h in air. All reactions were carried out in the liquid phase in a Teflon-coated stainless-steel batch reactor under continuous stirring. In a typical IP dehydration reaction, 16 g of isopropanol (Frutarom) and 60 mg of catalyst were loaded into the reactor and stirred at 473 K for 2 h. The products were analyzed after their separation from the catalysts, with the use of a HP 5890 gas chromatograph (Series II) fitted with a capillary column HP-1.

The synthesis of MTBE was carried out in the liquid phase as follows: 1.4 g of both methanol (Frutarom) and *t*-butanol (Aldrich) was loaded into a reactor, which was fol-

(a) Synthesis of MTBE

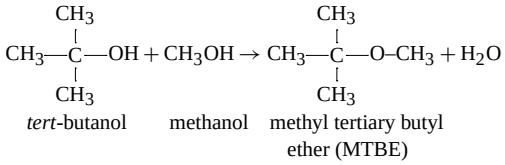

(b) Isopropanol dehydration

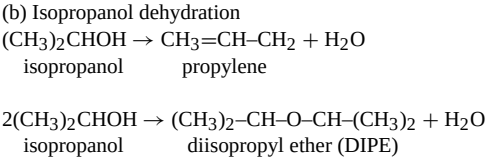

(c) Alkylation of catechol with *tert*-butanol

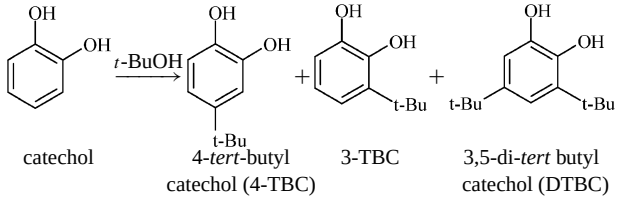

Fig. 1. The schemes of acid-catalyzed reactions selected for testing the $H_3PW_{12}O_{12}40$-based catalytic materials.

lowed by the addition of 30 mg of freshly activated catalyst. The reaction was carried out at 383 K for 2 h with continuous stirring. The products after separation from the catalysts were analyzed as in the case of the IP decomposition. Formation of isobutylene was negligible [11].

For the alkylation of catechol with *t*-butyl alcohol, 1.28 g of catechol (Aldrich) and 0.176 g of *t*-butyl alcohol (Aldrich) were added to 24 g of nitrobenzene (Aldrich). The mixture was loaded into the reactor, and the reaction was performed at 373 K for 1 h with continuous stirring after the addition of 80 mg of activated catalyst. The products, 3- and 4-*t*-butyl catechol (3- and 4-TBC) and 3,5-di-*t*-butyl catechol (3,5-DTBC), were analyzed with a gas chromatograph (HP 5890 Series II) with a HP-5 column.

The operating conditions were selected so as to limit the conversion with supported HPW catalysts to 30% to calculate the yield and turnover frequencies that reflect the intrinsic reaction rate. In the run time ranges used, the conversions increased proportionally, indicating that the reactions were kinetically controlled. The performance of the catalysts was characterized quantitatively by the yields (%Y) of the products and the product selectivities (%S) obtained at the selected conditions and was calculated as follows: $Y = (M_P/M_R) \times 100$; $S = (M_P/M_n) \times 100$, where M_P is moles of desired product, M_n is moles of all products obtained, and M_R is moles of loaded reagent (IP, methanol or catechol). The reaction turnover frequencies (TOFs, s^{-1}) were calculated as the number of moles of the corresponding reagents (*t*-BuOH, IP, or catechol) reacted (M_x) in a period of time per mol of HPW: $\text{TOF} = M_x/M_{\text{HPW}} \cdot \tau$, where M_{HPW} is moles of HPW loaded into the reactor, and τ is the reaction time in seconds. Constant conversion obtained by variation of the speed of agitation in the range of 600–900 rpm for MTBE synthesis and 700–1000 rpm for IP synthesis and *t*-butylation of catechol indicated the absence of external mass transfer limitation. A speed of agitation of 700 rpm for MTBE synthesis and 800 rpm for the other two reactions were chosen. In the absence of external mass transfer resistance, the reaction rate is directly proportional to catalyst loading [30]. Varying the catalyst loading in the range of 50–80 mg for IP dehydration, 20–40 mg for MTBE synthesis, and 70–100 mg for *t*-butylation of catechol resulted in linear changes in conversion, which indicated the absence of external diffusion limitations. Further experiments were carried out with catalyst loading as mentioned previously. The particle size variation in the range of 30–80 mesh did not affect the reaction rate, which indicates the exclusion of internal mass transfer limitations, and we chose the 40–60 mesh size for our measurements.

3. Results and discussion

3.1. Characterization of the HPW-alumina-grafted materials

As previously mentioned [24], grafting of SG with alumina made it possible to anchor HPW to the support without leaching in polar media and with minimal reduction of activity in acid-catalyzed reactions. However, the amount of alumina that can be grafted to SG is restricted, because of its limited surface area. Increasing the alumina content beyond 9 wt% by multistage grafting resulted in the formation of a bulk alumina phase. SBA-15 OMS with a higher surface area has the potential to increase the alumina content without the formation of alumina multilayers and hence to increase the HPW loading. The textural characteristics of parent and Al-grafted silica matrices and their chemical compositions (Si/Al ratios) are listed in Table 1. As can be seen from this table, the surface area and the pore volume of SG decrease with increasing alumina content (entries 1–4). This is consistent with the formation of an alumina layer, which does not contribute to the surface of the sample but contributes to the sample weight. The parent SBA-15 sample (entry 5) contained micropores ($d < 2$ nm) inside the mesopore walls,

Table 1
Chemical composition and surface area of alumina-grafted silica supports

Entry	Catalyst	Al_2O_3 (wt%)	Surface area (m^2/g)	Pore volume (m^3/g)	Avg. pore diameter (nm)
1	SG	–	362	1.3	13.7
2	AGSG-2	2.1	360	1.2	13.3
3	AGSG-8	8.3	348	1.2	13.7
4	AGSG-16	16.1	285	0.9	12.6
5	SBA-15	–	822	1.3	6.3
6	AGSBA-9	8.6	580	0.9	6.2
7	AGSBA-17	16.9	410	0.62	6.0
8	AGSBA-27	27.4	398	0.58	5.8
9	AGSBA-38	37.8	367	0.51	5.5

whose contribution to the total surface area, estimated by the *t*-plot method, was 145 m^2/g. The micropores disappeared already after insertion of 9 wt% of alumina. This explains the 30% decrease in the total surface area (from 822 to 580 m^2/g) due to blocking of the micropores with grafted alumina species. A further increase in alumina content in SBA-15 produced an additional reduction in surface area, reflecting mainly the increasing the sample weight and the extended formation of an alumina layer with minimal blocking of the mesopores. The pore diameter decreased by about 1 nm after repetitive grafting of both silicas (Table 1), indicating an increase in the thickness of the alumina layer.

The coverage of silica surface by grafted alumina was designated as partial, monolayer, and multilayer, based on experimental data reported in the literature [25]. With an excess concentration of Al *sec*-butoxide in toluene solution, a maximum coverage of ~ 8 and ~ 17 wt% of alumina was achieved on SG and SBA-15 supports, respectively. This was considered to be a monolayer coverage of silica surface with alumina. Accordingly, the alumina coverages in AGSG-2 and AGSBA-9 corresponding to lower alumina loadings were designated as partial or submonolayer coverage. Multilayer coverage of silica with alumina was achieved by further grafting of AGSG-8 and AGSBA-17 with alumina to yield AGSG-16 and AGSBA-27, respectively. We prepared the alumina-grafted SBA-15 material, AGSBA-38, by repeating the grafting procedure on AGSBA-27.

Anchoring of HPW was done with the addition of various supports to a methanolic solution of HPW. The HPW loading and the textural characteristics of the supported materials are summarized in Table 2. As expected, pure silica did not adsorb HPW from the methanolic solution. It was removed from the pores at the washing stage of the sample preparation, leaving the matrices texture unchanged (entries 1 and 2). Fixation of HPW in the pure silica matrix could be achieved only by exclusion of the washing stage after impregnation. In the case of SG, a composite material with 19 wt% HPW was prepared, and it showed a reduced surface area and pore volume relative to the parent support (entry 3). HPW was strongly adsorbed to the pure alumina, yielding a material with 29 wt% HPW, and the surface area and pore volume were reduced according to the increase in the sample weight (Table 2, entry 4). Grafting of alumina to both silica matrices resulted in a strong adsorption of HPW from the methanolic solution that could not be removed by washing. The amount of HPW adsorbed from a methanolic solution, containing an excess of the acid (enough to achieve a loading of 60 wt% HPW after adsorption), increased with increasing alumina content, making it possible to load AGSG in the range of 5–21 wt% and AGSBA in the range of 21–35 wt%. The adsorption of HPW changed the textural parameters (surface area and pore volume normalized per gram of the material) of the alumina-grafted supports in a way that reflected only the matrix dilution with HPW. This could be the result of strong adsorption of HPW in the form of isolated molecular species that do not block the pores and do not contribute to the surface area of the alumina-grafted supports.

Table 2
Chemical composition and surface area of supported HPW catalysts

Entry	Catalyst	HPW loading (wt%)	Surface area (m^2/g)	Pore volume (m^3/g)	Avg. pore diameter (nm)
1	HPW/SG	< 0.5	350	1.3	14.8
2	HPW/SBA	< 0.5	830	1.3	6.3
3	HPW/SG	19	238	0.85	14.3
4	HPW/Al_2O_3	29	200	0.54	10.8
5	HPW/AGSG-2	5	242	0.78	13.2
6	HPW/AGSG-8	19	220	0.64	12.5
7	HPW/AGSG-16	21	211	0.64	12.1
8	HPW/AGSBA-9	21	480	0.77	6.4
9	HPW/AGSBA-17	29	370	0.55	5.9
10	HPW/AGSBA-27	31	316	0.44	5.5
11	HPW/AGSBA-38	35	269	0.36	5.3

3.2. Immobilization of HPW on AGSG and AGSBA and its catalytic performance

The catalysts listed in Table 2 were used in three representative acid-catalyzed reactions (Fig. 1); the results of the catalytic tests are presented in Table 3 and Fig. 2. First we examined the effect of the amount of alumina loaded by grafting on both silica matrices on product yields (Fig. 2). It was found that the activity of the HPW catalysts supported on AGSG and AGSBA in all three acid-catalyzed reactions passed through a maximum with increasing alumina content. These maxima at 8 wt% alumina in SG and at 17 wt% alumina in SBA-15 correspond to the maximum amounts of alumina that can possibly be adsorbed in one step. This means that the activity increases with increasing alumina content, up to its full coverage of the silica surface. Moreover, at higher alumina loadings, achieved by multistage grafting, although the HPW loading was increased, the activities of the catalysts on both silica supports decreased for all three reactions (Fig. 2). This can be explained by the

Table 3
Testing results of bulk and supported HPW catalysts

Entry	Catalyst	IP dehydration[a] DIPE yield (%)	MTBE synthesis[b] MTBE yield (%)	*t*-Butylation of catechol[c] 4-TBC yield (%)
1	HPW	33 (3.6[d])	77 (13.2[d])	47 (20.7[d])
2	HPW/Al_2O_3	4 (1.1[d])	12 (5.5[d])	1.3 (0.6[d])
3	HPW/AGSG-8	9 (2.6[d])	24 (13.6[d])	16 (11.3[d])
4	HPW/AGSBA-17	12 (2.8[d])	35 (14[d])	27 (11.3[d])

[a] Reaction conditions: 16 g IP, 60 mg catalyst, 437 K, 2 h. The selectivity to propene was 20% for all the catalysts.
[b] Reaction conditions: 1.4 g methanol, 1.4 g *t*-butanol, 30 mg catalyst, 383 K, 2 h.
[c] Reaction conditions: 24 g nitrobenzene, 1.28 g catechol, 0.176 g *t*-butanol, 80 mg catalyst, 373 K, 1 h.
[d] TOF (s^{-1}).

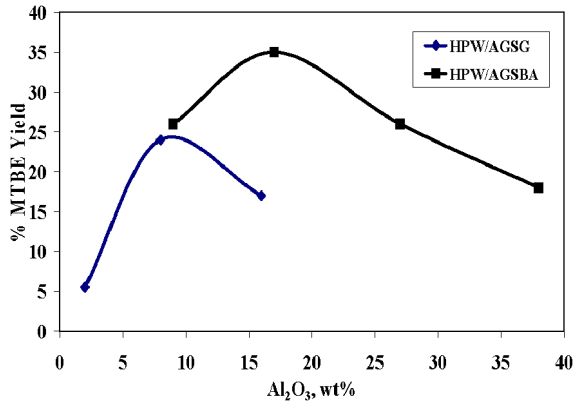

(a)

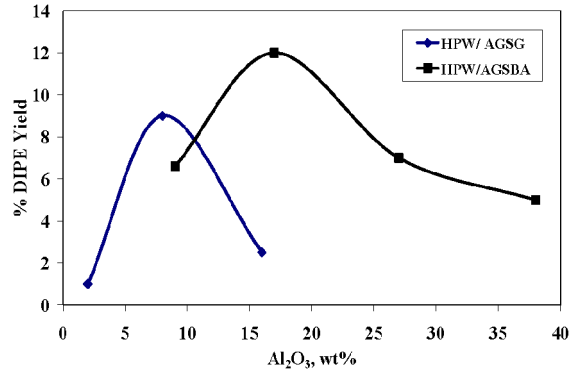

(b)

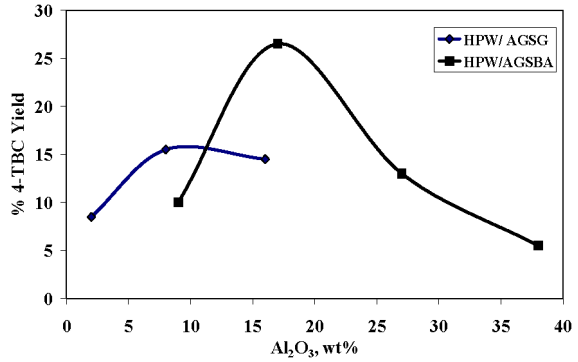

(c)

Fig. 2. Effect of alumina loading in silica-gel and mesostructured SBA-15 silica on the yields of products of catalytic reactions measured at standard conditions with $H_3PW_{12}O_{40}$ immobilized on these silicas: (a) condensation of methanol with *t*-butanol; (b) dehydration of isopropanol; (c) alkylation of catechol with *t*-butanol.

formation of a bulk-like alumina phase that at high alumina loadings affects the acidity of HPW, as in the case of pure alumina. MTBE was the only product of the *t*-BuOH and MeOH condensation reaction. The selectivity for DIPE in IP dehydration was ∼ 80%, and the selectivity for 4-TBC in the *t*-butylation of catechol was ∼ 75% for all of the catalysts, suggesting that it is determined only by the nature of active HPW catalytic material. The yields of MTBE, DIPE, and 4-TBC measured under the same conditions with alumina-grafted silica matrices in the absence of HPW at all alumina loadings were less than 0.5%. This allows us to attribute the activities of supported HPW catalysts exclusively to the adsorbed acid.

As expected, HPW/Al_2O_3 displayed the lowest yields of products in all of the tested reactions (Table 3, entry 2) [24]. The reaction turnover numbers measured with the HPW catalyst supported on pure alumina were 2.5 to 19 times lower than with HPW adsorbed to silicas grafted with alumina at nearly full coverage, depending on the testing reaction. At the optimal alumina loading levels, similar reaction turnover numbers were measured with HPW supported on AGSG-8 and AGSBA-17 (Table 3), and the yields of the products obtained over the HPW/AGSBA-17 were 1.3 to 1.7 higher than over HPW/AGSG-8, depending on the testing reaction. Pure HPW that works as a homogeneous catalyst (Table 3, entry 1) displayed reaction turnover numbers equal to (for MTBE) or 1.3 times higher than (for IP dehydration) or 1.8 times higher than (for catechol alkylation) HPW anchored to alumina-grafted silicas (Table 3, entries 3 and 4). Thus the specific activity of HPW in terms of TOF varies in the following order:

$$\text{HPW} \geqslant \text{HPW/AGSG-8} = \text{HPW/AGSBA-17} \gg \text{HPW/Al}_2\text{O}_3.$$

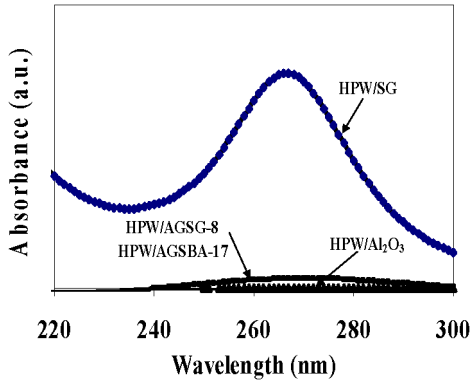

Fig. 3. UV–vis spectra of methanol filtrate after washing the supported $H_3PW_{12}O_{40}$ samples.

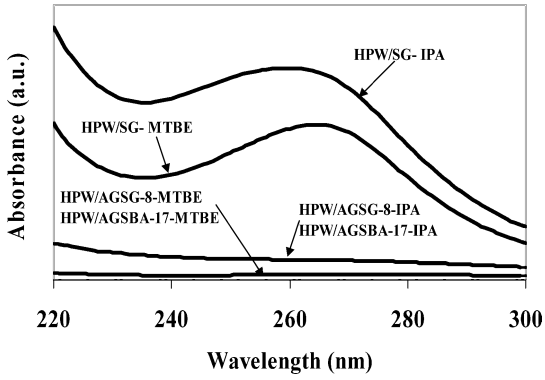

Fig. 4. UV–vis spectra of product mixtures after conducting MTBE synthesis and isopropanol dehydration and catalyst separation.

The leaching of the HPW from the various supports was studied by UV–visible spectroscopy (Figs. 3 and 4). Mixing of the catalysts, which were prepared by dispersion of HPW in alumina-free SG by evaporation (Table 2, entry 3), in 20 cm^3 of methanol at room temperature for 3 h resulted in a complete removal of HPW from the support. The evidence for this is the appearance of a strong signal in the UV–visible spectra at $\lambda = 267$ nm, which is characteristic for HPW in solution (Fig. 3). Similar treatments for HPW/AGSG-8, HPW/AGSBA-17, and HPW/Al_2O_3 catalysts, followed by chemical analysis after the treatment and by recording of UV–visible spectra for the methanol filtrate (Fig. 3), showed no leaching of HPW from the catalysts. This confirms strong immobilization of HPW on these supports. UV–visible spectra for the reaction mixtures, obtained after the MTBE synthesis and IP dehydration experiments with HPW supported on alumina-free silica gel, AGSG-8, and AGSBA-17 after catalyst separation, are shown in Fig. 4. Under these reaction conditions, the HPW leached out completely from pure SG but remained immobilized on the alumina-grafted silicas. This was also confirmed by chemical analysis of the spent catalysts. In conclusion, we can thus be certain that grafting the silica surface with alumina results in efficient immobilization of HPW, which maintains its high activity in acid-catalyzed reactions.

3.3. Characterization of the catalysts

As previously shown, HPW supported on both alumina-grafted silica and alumina supports was strongly immobilized; however, the catalytic performances were different. In addition, grafting of alumina in multilayers to silica supports, before immobilization of HPW, also resulted in low catalytic activity of the corresponding catalysts. This could be attributed to two different phenomena. Grafting could create alumina surface sites with a basicity strength that is lower than that of the sites of pure alumina or alumina multilayer, hence increasing the surface acidity of the adsorbed HPW. Alternatively, different sizes of alumina particles could lead to differences in the acidity of HPW. Whereas the density of available binding sites for HPW at the surface of pure alumina is high, because of the large-size alumina particles, the smaller clusters of grafted alumina yield a lower density of basic sites at the silica surface, hence reducing the overall HPW binding. This can decrease the extent of neutralization of the acid sites in the adsorbed Keggin species. Apparently, the two phenomena could take place simultaneously. To clarify the effects of alumina grafting on the basicity of the supports, the binding characteristics relative to HPW, and the acidity of adsorbed HPW species, we applied a set of analytic and spectroscopic techniques to all of the catalysts discussed above.

3.3.1. Silica and alumina grafted silica supports

It is generally accepted that the basic strength of the sites located at the surface of metal oxides is determined by the average charge on the oxygen atoms, which can be calculated from Sanderson's theory of electronegativity [31,32], by the electronegativity equalization method [33–35]. It was previously demonstrated that the temperature required for desorption of CO_2 from basic surface sites (decarbonation) increases linearly with the value of the negative charge on the oxygen atoms [35]. In addition, the binding energy of O 1s electrons, measured by XPS, was found to decrease with increasing negative charge on the surface oxygens [36]. Therefore, to validate the nature of the grafted alumina phase and verify whether the grafted alumina sites at the silica surface display lower basicity strength than that at the surface of pure alumina, we applied FTIR, XPS, and CO_2-TPD methods to our samples.

3.3.1.1. FTIR of alumina grafted silicas FTIR spectra for SG, SBA-15, pure alumina, and the alumina-grafted silica supports in the region of 400–1400 cm^{-1} are shown in Fig. 5. Bands centered at 1095, 807, and 470 cm^{-1} are attributed to the asymmetric stretching, symmetric stretching, and bending modes of Si–O–Si, and the band at 967 cm^{-1} in the case of SBA-15 and the shoulder in the same region for SG are characteristic of the stretching vibration of Si–OH [37–40]. For alumina, all of the characteristic bands in the 500–700 cm^{-1} region, assigned to AlO_6 condensed groups and complex AlO_4 and AlO_6 interactive vibration symmetric stretching modes, are present [41]. The preparation procedure employed in this study envisages binding of alumina species to the silica surface via the surface silanols. Indeed, the intensity of the Si–OH vibration in silica supports became substantially lower after its grafting with alumina. It can clearly be observed that the band at 967 cm^{-1}, present in the spectra of parent SBA-15, and the weak shoulder observed in this region in the spectra of SG are sup-

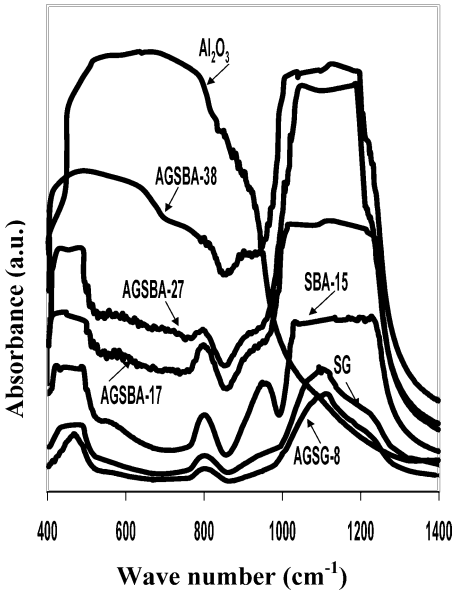

Fig. 5. FTIR spectra of silica-gel, alumina, SBA-15 and alumina-grafted silica supports.

pressed after grafting with alumina (in the AGSBA-17 and AGSG-8 samples). This confirms that grafting of alumina at the silica surface indeed occurs via the silanol groups. It can also be observed that the vibration features of alumina in AGSBA-38 in the 500–800 cm^{-1} region become dominant because of the formation of a bulk-like alumina phase. On the other hand, identical vibration features in the spectra of the AGSG-8 and AGSBA-17 materials and of SG and SBA-15, respectively, were observed in this spectral region. This points to the presence of small isolated alumina clusters at partial and full coverage and the formation of a bulk-like alumina phase inside the silica pores after multistage grafting.

3.3.1.2. XPS of alumina-grafted silicas XPS spectra representing the core level of the O 1s region in pure alumina, SG, and the two alumina-grafted supports, AGSG-8 and AGSBA-17, are shown in Fig. 6. The distribution of O 1s BE of the electrons for alumina-grafted silicas in the range of 528–535 eV is substantially different from that measured for pure silica and alumina (Fig. 6a). In contrast to the peaks centered at 532 eV for alumina-grafted silicas, the peaks of alumina and SG are centered at 531.4 and 532.5 eV, respectively, in agreement with the data obtained by Prado et al. [42]. This reflects a higher basicity of the surface oxygen atoms on alumina relative to SG. Grafting of SG (Fig. 6b) or SBA-15 (Fig. 6c) with alumina at nearly full coverage shifted the position of the peak to lower BE values that could reflect the increase in surface basicity. But deconvolution of the spectra obtained with both AGSG-8 and AGSBA-17 composites yielded two peaks centered at the same positions as in SG and pure alumina within the accuracy of the instrument. This is an indication of the formation of basic sites with the same basic strength on alumina-grafted silicas as on the surface of pure alumina. The Al/Si ratios of the surface layer of AGSG-8 and AGSBA-17 measured by XPS were 0.37 and 0.58, respectively, versus 0.05 and 0.13 from the bulk EDS analysis. This reveals high dispersion of the alumina phase and thus the location of most of the grafted alumina in the surface layer of the material after calcination at 773 K. Under such treatment conditions, diffusion of aluminum into the silica matrix is not feasible since it is reported to occur at temperatures greater than 1000 K, from the shift in O 1s BE [42].

3.3.1.3. CO_2-TPD on alumina-grafted silicas The data from CO_2-TPD experiments were also consistent with the conclusion that the basicity of the sites at the silica surface after grafting with alumina and the sites at the surface of pure alumina are similar (Fig. 7). Whereas pure silica supports, SBA-15 and SG, do not bind CO_2 at temperatures greater than 200 °C (not shown), insertion of alumina by grafting creates basic sites retaining CO_2 up to 550 °C. The distributions of relative intensities of CO_2 signals, normalized per square meter of material, in a wide temperature range of 100–550 °C (the shape of TPD spectra) are similar for the alumina-grafted silicas and for pure Al_2O_3. This implies a similarity between the distributions of surface basic sites, in terms of their basic strength, in grafted silicas and pure alumina. The main difference lies in the surface concentration (per square meter) of these basic sites, derived from the integrated intensities of the CO_2 evolution peaks in the range of 100–550 °C. This increased in the following order: AGSG-8 < AGSBA-17 ≪ Al_2O_3 at ratios 1:1.6:10. The higher concentration of basic sites in AGSBA-17 compared with AGSG-8 (inset in Fig. 7) is consistent with the substantially elevated intensity of the band at 967 cm^{-1} in IR spectra. This is due to the enhanced concentration of silanols in SBA-15 relative to that in SG, as measured by IR (Fig. 5), with the higher Al/Si ratio in the surface layer of

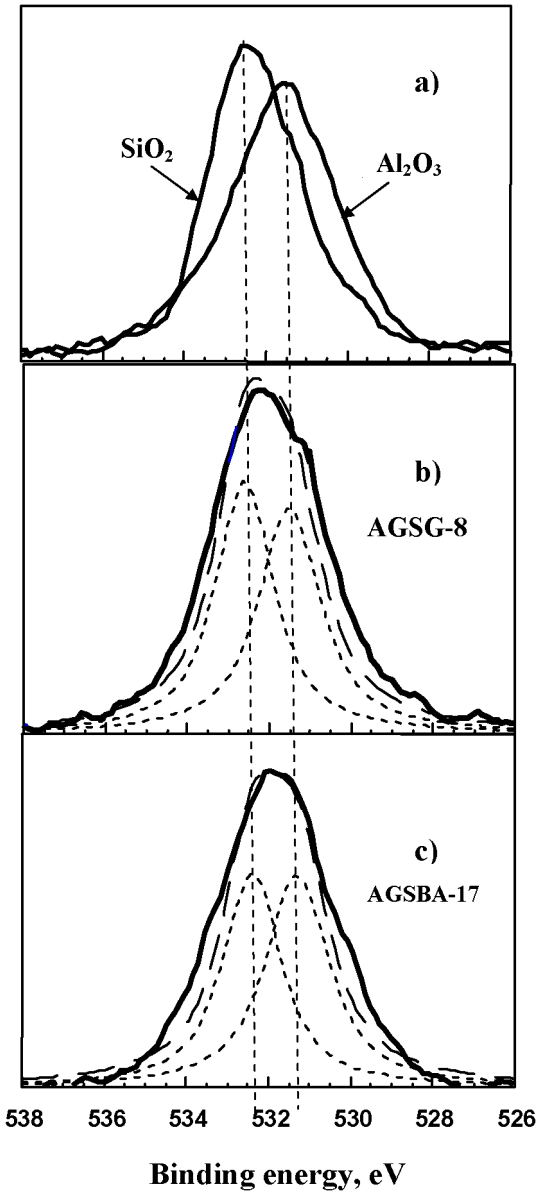

Fig. 6. XPS spectra of the core level of O 1s region recorded with pure silica-gel and alumina (a), alumina-grafted silica-gel AGSG-8 (b) and alumina grafted SBA-15 AGSBA-17 (c).

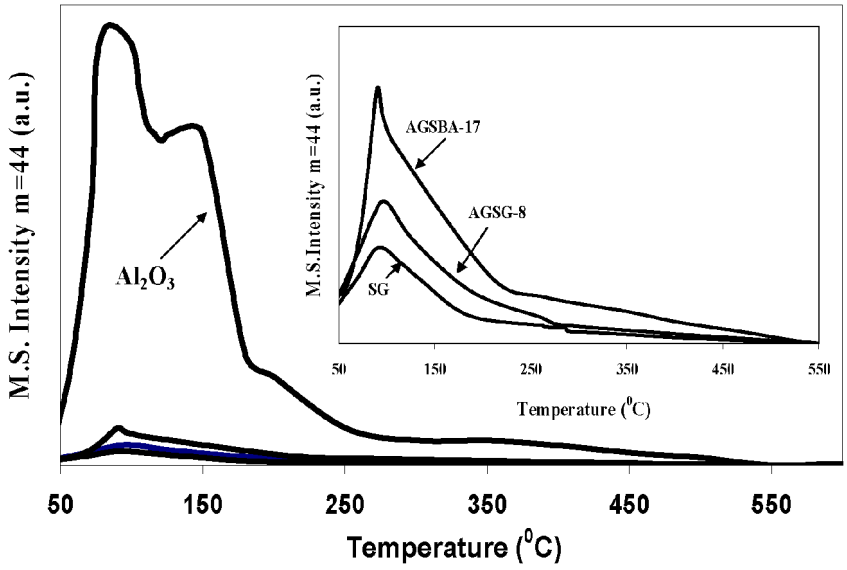

Fig. 7. The CO_2-TPD spectra recorded with pure silica, alumina, alumina-grafted silica-gel (AGSG-8) and alumina-grafted SBA-15 (AGSBA-17).

AGSBA-17 than in AGSG-8, measured by XPS. This is directly connected with the higher surface concentration (per square meter) of grafted alumina in AGSBA-17 relative to AGSG-8 (Table 1).

From TPD of CO_2, XPS, and FTIR studies on alumina-grafted silicas it can be envisaged that the grafted alumina species exhibit basic sites with the strengths like those observed with bulk alumina. However, at nearly full coverage of alumina on silica surface in AGSG-8 and AGSBA-17 supports, the surface concentration of basic sites is ~ 10 times lower than in bulk alumina. This means lower local concentration of basic sites in alumina-grafted silicas at partial and nearly complete alumina coverage, relative to the pure alumina phase.

3.3.2. State of immobilized HPW

3.3.2.1. XRD of HPW-containing samples XRD patterns of pure-HPW reference samples in hydrated (as received) and anhydrous (after heating at 200 °C for 2 h in air) forms and of HPW deposited on SG, alumina, and alumina-grafted silica supports are shown in Fig. 8. The XRD pattern of the dehydrated HPW sample corresponds to a cubic structure (space group Pn3m no. 224) with $a = 12.165 \pm 0.001$ Å, in agreement with ICDD card no. 75-2125. The pattern of the diffractogram recorded for the hydrated HPW sample was close to that given in ICDD card no. 50-655. This is characteristic for an orthorhombic structure with 21 water molecules per Keggin molecule. It includes three groups of reflections centered at $2\theta = 8°$ ($d = 11.0$ Å), $2\theta = 19°$ ($d = 4.7$ Å), and $2\theta = 28°$ ($d = 3.2$ Å). In both hydrated and dehydrated HPW materials the widths of the reflections indicate that the crystal domain sizes are large, greater than 50 nm.

After deposition of HPW on SG by impregnation without washing (Table 2, entry 3), the diffractogram displayed a wide peak at $2\theta = 23°$, corresponding to amorphous silica,

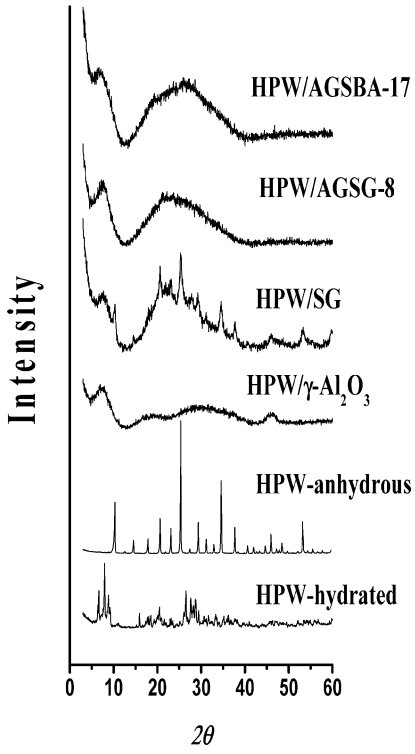

Fig. 8. XRD patterns of bulk and supported $H_3PW_{12}O_{40}$ materials.

a series of relatively narrow reflections in the range 10.3°–57.8°, matching the patterns of the dehydrated cubic HPW phase with a crystal domain size of 20 nm, and a wide peak at $2\theta = 8°$ ($d = 11.0$ Å). The last reflection could be attributed to the X-ray scattering by nonordered hydrated polyanions of HPW that are present at the surface as isolated molecular moieties or small clusters containing few Keggin units with crystal domain sizes of 2.3 nm measured from the broadening of this peak. The absence of visible reflections at higher angles that could be attributed to hydrated HPW structures

indicates a deficiency of the short-range order in these clusters. Although the number of water molecules in such clusters is not known, it could be supposed that a cluster with a diameter of 2.2–2.5 nm that contains less than 5 Keggin units can include more hydrogen-bonded water molecules per unit relative to bulk HPW. This is due to the higher accessibility of HPW protons in such clusters and corresponds to substantially higher Keggin hydration. Deposition of HPW on pure alumina (Table 2, entry 4) yielded a XRD pattern that exhibits reflections from the alumina phase corresponding to a d spacing of 4.6, 2.4, 1.97, and 1.40 Å and one wide peak centered at $2\theta = 8°$. It is a result of a strong interaction of the HPW with the basic sites present at high concentration at the surface of alumina that stabilizes the HPW phase only in the form of hydrated surface molecular species. We observed a similar picture by recording XRD patterns of HPW adsorbed on alumina-grafted silicas with an alumina content corresponding to nearly full coverage (Fig. 8).

Thus the XRD data offer evidence for the existence of HPW adsorbed to pure alumina and to the alumina-grafted silicas in the form of hydrated surface molecular species or small clusters containing few Keggin units with higher hydration levels than in the bulk HPW. However, no information can be gained from XRD about their molecular structure. To clarify the structural integrity of the Keggin after the adsorption/deposition on supports, and to ascertain how immobilization affected the acidity of HPW, we conducted additional FTIR, MAS NMR, and NH_3-TPD investigations.

3.3.2.2. FTIR of HPW-containing samples FTIR spectra for hydrated bulk HPW and HPW supported on alumina-grafted silicas are shown in Fig. 9. The bands of the bulk HPW sample appearing at 1082, 983, 886, 793, 595 (weak), and 521 (weak) cm^{-1} can be assigned to the characteristic Keggin anion vibrations of ν_{as}(P–O), terminal ν_{as}(W=O), ν_{as}(W–O_b–W), ν_{as}(W–O_c–W), δ(O–P–O), and ν_s(W–O–W), respectively [7,43–46]. The subscripts b and c indicate corner-sharing and edge-sharing oxygen, respectively, and the W–O–W bridges belong to the WO_6 octahedra. In all of the samples containing HPW supported on silica, the bands 1082, 983, and 793 cm^{-1} characteristic for HPW were masked by matching bands of silica supports [5,37,46,47]. The weak bands attributed to HPW at < 600 cm^{-1} fail to appear, because of low concentration of HPW due to its dilution by silica. A broad shoulder in the region of 886 cm^{-1} that is observed for HPW deposited in all alumina-grafted silica supports is a characteristic vibration mode, ν_{as}(W–O_b–W), of HPW. The absence of prominent shift in the position of this peak, relative to the bulk HPW, suggests that HPW retains its Keggin structure after immobilization at the surface of alumina-grafted silicas. For HPW/Al_2O_3 the characteristic peaks of HPW between 700 and 1000 cm^{-1} that are more sensitive to interactions with the support surface were not observed, because of intense absorption by alumina in this region [7]. Thus no information can be gained from this spectral region on the structure

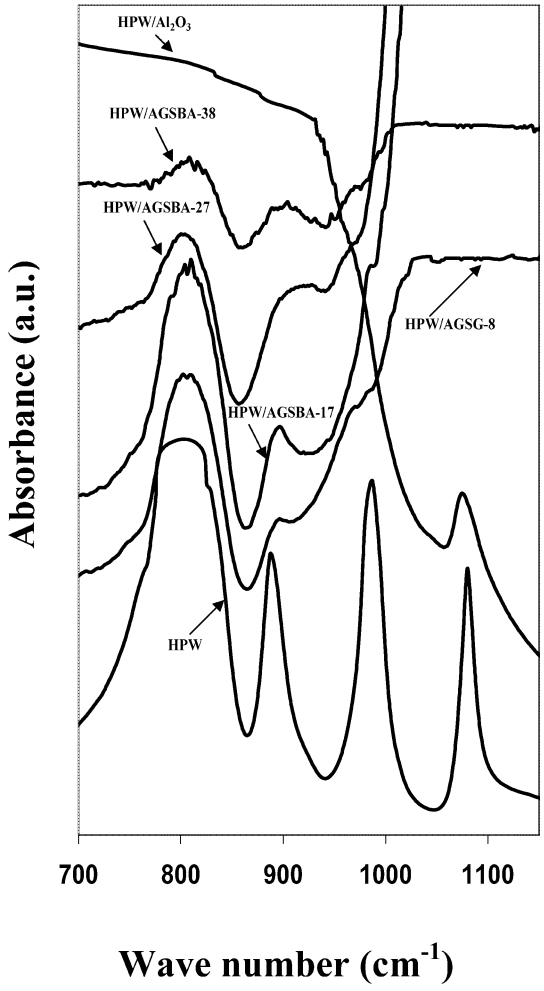

Fig. 9. FTIR spectra of bulk and supported $H_3PW_{12}O_{40}$ materials.

of Keggins strongly interacting with the basic sites of pure alumina. A broad band centered at 1082 cm^{-1} and assigned to the symmetric vibration of P–O indicates that HPW retains the Keggin structure on alumina, since the appearance of a lacunary (defect) Keggin anions causes this band to split into two components at 1087 and 1055 cm^{-1} [19,48]. However, the peak broadening and tailing suggest a degree of structural distortion of the Keggin.

It is well known that HPW undergoes partial decomposition to form lacunary and/or dimeric species during catalyst preparation and pretreatment [7,11,19,43,48–50]. Partial decomposition of HPW occurs in aqueous solution when the pH exceeds 1.8, and it has been shown that the limiting concentration of HPW, below which it undergoes partial decomposition, is ~ 7 wt% for water and ~ 1 wt% for methanol [49]. We have used a methanol solution of HPW with a concentration of 18 wt% that retained the HPW Keggin structure during our catalyst preparation. Lacunary and/or dimeric species of HPW can also form at the surface of the support as a result of the Keggin's thermal degradation during pretreatment at temperatures equal to above 350 °C [11,48,49]. The catalysts in our study were pretreated at 200 °C,

thus ruling out the possibility of thermal decomposition of the Keggin structure.

3.3.2.3. NMR of HPW containing catalysts In the supported HPW systems employed in this study, two types of protons can be envisaged, namely, "free" (or acidic) protons delocalized among the Keggins and "bound" protons that are localized between the Keggins and the support because of strong interaction with the surface basic sites. ^{1}H and ^{31}P MAS NMR studies were carried out to obtain information about the structure and mode of binding of adsorbed HPW species to the basic sites of the support and to characterize the "free" protons as their Brønsted acidic sites.

The ^{1}H MAS NMR chemical shifts of highly acidic protons are more positive and have been observed in zeolites wherein the OH groups are visualized as being static [51]. However, in HPW-based materials the relationship between acidic strength and proton chemical shifts is not straightforward, because of the high mobility of protons arising as a result of hydrogen bonding with water molecules [52,53]. From the temperature dependency of line-widths and chemical shifts in a ^{1}H MAS NMR study on a reduced silver salt of HPW in the presence of hydrogen, protonic chemical shifts observed at 6.4 and 9.3 ppm were ascribed to "mobile" and "non-mobile" protons, respectively [53]. The protonic chemical shifts of supported HPW move upfield relative to the bulk HPW to the position at ~ 5 ppm at low loadings (< 40 wt%), whereas at higher loadings the peaks shifted downfield to a position of ~ 8 ppm, similar to the bulk HPW [54–56]. However, free and bound protons of the acid have not been distinguished. This could be due to the presence of different kinds of proton sources, such as surface hydroxyls, structural and free water, and acidic protons accompanied by fast exchange of protons among them. Similar to the data reported in the literature, it was impossible to distinguish between "free" and "bound" protons in the small clusters of supported HPW materials prepared in this study based on the ^{1}H MAS NMR spectra recorded at room temperature (not shown) for reasons that are outlined above.

In contrast to this, in ^{31}P MAS NMR spectra, the interpretation of which does not suffer from the limitations mentioned above, the effects of "free" and "bound" protons on the ^{31}P chemical shifts of the Keggin should be significant, yielding information about the structure and bonding mode of HPW moieties. The results of the single $\pi/2$ pulse ^{31}P MAS NMR experiments on hydrated pure-HPW and supported HPW catalysts are shown in Fig. 10. Only the center band regions of the spectra are shown, since the sidebands were generally very weak. All spectra could be characterized in terms of three spectral bands with varying relative intensities. The sensitivity of the central-^{31}P chemical shift values of the Keggin units to changes in the HPW structure has been discussed extensively in the literature [54,57,58]. Different hydration levels of HPW resulted in distinct changes in the NMR spectra. Chemical shift values between -16 ppm and -11 ppm were reported in a variety of studies and correlated

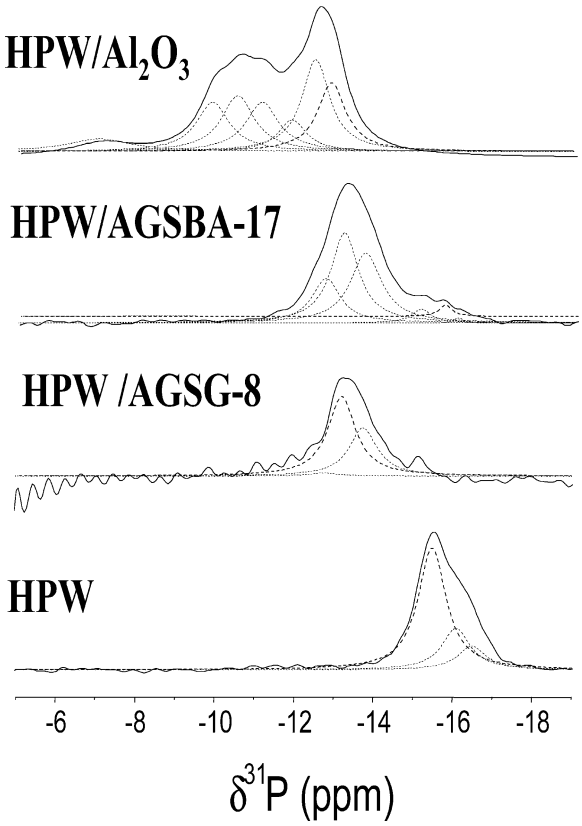

Fig. 10. ^{31}P MAS NMR spectra of bulk and supported $H_3PW_{12}O_{40}$ materials.

to the positively charged $\{H^{+}kH_2O\}$ ($k = 0, 1, 2$) moieties connecting the $(PW_{12}O_{40})^{3-}$ anions in crystalline materials. Whereas for a hydrated sample with $k = 2$ a chemical shift of about -15.5 ppm was found, the anhydrous samples with $k = 0$ showed a line around -11 ppm [7,11,37,50,59]. Thus the source of the changes in the chemical shift at the center nucleus of the Keggin anions is correlated to the average proximity of their compensating charges. One isotropic line in a ^{31}P MAS spectrum of a HPW powder sample indicated that, over a certain time scale, all phosphorous nuclei experience the same averaged chemical environment, presumably due to proton exchange. On the other hand, when Keggin units are located close to crystal surfaces or defects, one would expect that their chemical shift values are different from the bulk value.

Inspection of the ^{31}P spectrum of our hydrated bulk-HPW sample (prepared by recrystallization from water and calcined at 473 K for 2 h in air) revealed that the spectral band around -16 ppm is composed of several lines. Deconvolution of this band, assuming Lorentzian line shapes, results in three resonances, at -15.5 ppm (65%), -16.1 ppm (22%), and -16.6 ppm (13%), where relative integrated intensities are given in parentheses (Fig. 10a). The most intense line must be assigned, according to the literature, to hexahydrated HPW with $k = 2$, wherein the protons are delocalized among the Keggins. The other high-field shifted lines could be attributed to Keggins that experience a distortion in their

hexahydrated coordination due to defects or surface effects. The relative intensities of the three lines are then an indication of the size of the crystalline particles. No efforts were made to improve the homogeneity or size of the crystalline material by recrystallization, since the supported HPW samples were treated in a similar manner.

In the spectra of HPW supported on AGSG-8 and AGSBA-17, the ^{31}P band is shifted to a lower field and the relative intensities of the three components are significantly different from the lines in the bulk-HPW band. The HPW/AGSG-8 sample gave a spectrum consisting of three components positioned at −12.8 ppm (2%), −13.2 ppm (61%), and −13.8 ppm (37%), and the HPW/AGSBA-17 sample showed lines at −12.8 ppm (19%), −13.2 ppm (39%), and −13.8 ppm (34%), again with relative intensities given in parentheses. These samples were dried at 473 K for 2 h before the measurement.

The downfield shifts to −10 to −14 ppm of the ^{31}P MAS NMR signal in supported HPW materials relative to the bulk have been attributed to three types of species: (a) species $[(SiOH_2)^+(H_2PW_{12}O_{40})^-]$ arising from interaction of HPW with the support surface [48–50]; (b) lacunary and/or dimeric species arising as a result of partial decomposition of HPW [7,48–50]; and (c) HPW species differing in hydration levels [37,43,60]. In the studies attributing the downfield shifts to lacunary and/or dimeric species of HPW, it is more often the case that the partial decomposition of HPW had occurred at the preparation stage, in solution at low HPW concentrations and/or because of the thermal degradation at high pretreatment temperature [7,48–50]. As discussed earlier, the preparation and pretreatment conditions employed in our study ensured the stability of the Keggin structure. The formation of species of types (a) and (c) results in the localization of protons, thereby increasing their proximity to the Keggin anion because of the decrease in proton mobility.

The position of the band around −13 ppm observed in HPW supported on alumina-grafted silicas is similar to that in the spectra obtained for a bulk HPW sample with $k = 1$ corresponding to a dihydrate of HPW [58]. The shift must then be attributed to the interaction of adsorbed HPW particles with the grafted alumina, since FTIR spectra have revealed the integrity of the Keggin structure of immobilized HPW. The protons of HPW interact with the basic sites of alumina, leading to their localization, and an increased averaged proximity to the Keggins is achieved. This increase in proximity causes a downfield movement of the ^{31}P NMR chemical shifts. The relative line intensity distribution inside the spectral bands of the HPW particles shows a significant reduction of the line at −12.8 ppm characteristic for Keggins located in the bulk of the HPW crystals. This suggests that the adsorbed HPW shows a much shorter crystal correlation than that in the bulk sample and therefore is composed of small HPW particles. This is in agreement with the XRD data wherein only long-range order was observed in the supported HPW phase, revealing the molecular character of adsorbed HPW species.

The HPW/Al_2O_3 sample showed two spectral bands around −12.5 and −10.5 ppm. Both of these bands are at lower field than for the HPW supported on alumina-grafted silicas. The distinction between the −12.5 and −13.2 ppm bands is significant, indicating that there is a difference between the modes of binding of HPW to pure alumina and alumina grafted to a silica surface. The reason for this difference can be explained by the increased basicity of the pure alumina. The additional shift to −10.5 ppm shows the presence of more binding options for the protons on an Al_2O_3 surface due to an increase in the concentration of the basic sites. This causes the localization of more protons and hence their greater proximity to the Keggins, similar to the $k = 0$ state in dehydrated HPW, which is attributed to an increase in the number of protons localized on the Keggin [58]. Such a strong interaction of HPW with the alumina surface is also additionally confirmed by the broad peak at 1080 cm^{-1} in the FTIR spectra (Fig. 9), indicating structural distortion of the Keggin. Thus the higher magnitude of the ^{31}P NMR downfield shifts in HPW/Al_2O_3 compared with HPW supported on alumina-grafted silicas arises because of the interaction of a larger number of protons with the basic sites.

3.3.2.4. NH_3-TPD of HPW-containing catalysts The NH_3-TPD spectra recorded for HPW/Al_2O_3 and the two HPW catalysts supported on AGSG-8 and AGSBA-17 materials are shown in Fig. 11. The intensities of the m.s. signals are normalized per gram of heteropolyacid in order to compare the intrinsic acidity of the catalytic phase. The TPD spectra show similar amounts of ammonia desorbed per gram of molecular HPW species immobilized by grafted alumina species at the surfaces of SG (AGSG-8) and SBA-15 (AGSBA-17). These samples displayed similar distributions of the amount of base desorbed in the range between 250 and 600 °C, reflecting similar acidity strengths of the protonic sites. The HPW adsorbed on pure alumina retained half as much ammonia, estimated from the integral intensities of the NH_3-TPD peaks in the temperature range of 250–550 °C. The HPW immobilized on the surface of pure alumina exhibited a different distribution of acid sites according to their acidity strength: no ammonia was retained by HPW/Al_2O_3 at $T > 550$ °C, whereas a significant amount of base was withheld at $T > 550$ °C by HPW/AGSBA-17 and HPW/AGSG-8 catalysts. Analogous trends, with integrated intensities and shapes of the TPD peaks close to those recorded with HPW/Al_2O_3, were observed for the HPW/AGSG-16 and HPW/AGSBA-38 catalysts (not shown), where HPW was immobilized at the surface of a bulk-like alumina layer. These NH_3-TPD data therefore show that the strong adsorption of HPW molecules at the surface of bulk alumina or bulk-like alumina layers causes a significant neutralization of their acidity and thus a reduction in the number of available acid sites, especially those with the highest acidity strength. It can be concluded that HPW adsorbed on small alumina clusters grafted to a

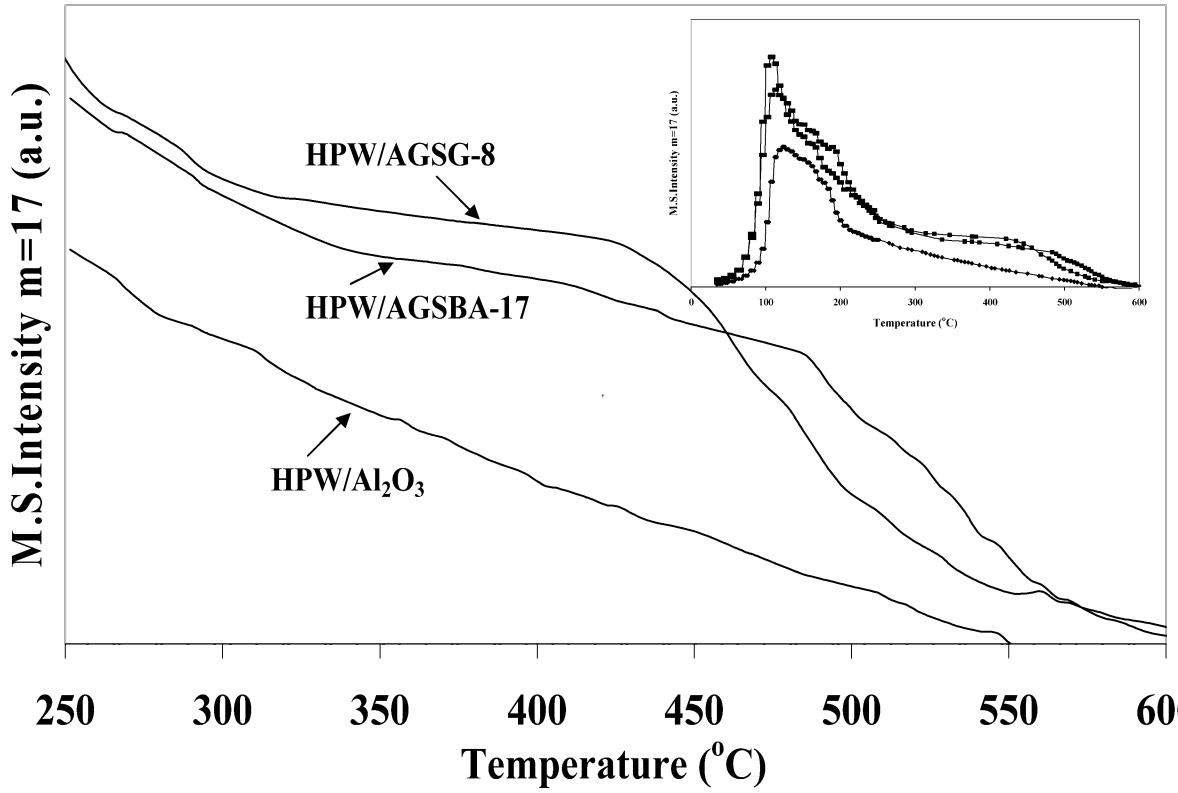

Fig. 11. NH_3-TPD spectra recorded with $H_3PW_{12}O_{40}$ immobilized at different supports.

silica surface preserves its acidity to a much higher extent than it does when it is bound to the bulk alumina.

3.4. Mechanism of HPW immobilization at an Al-grafted silica surface

Based on the information that was collected about the state and the basicity/acidity of the supports and the HPW catalytic phase, a distinct mechanism of HPW immobilization at the pure alumina and alumina-grafted silica surfaces is proposed. The high surface concentration of basic sites in Al_2O_3 and alumina-grafted silicas covered with a bulk-like alumina layer (CO_2-TPD) resulted in a high level of heteropolyanions distortion (^{31}P MAS NMR, FTIR) and substantially low acidity and the disappearance of acid sites of high acidity strength in the corresponding HPW/support materials (^{1}H MAS NMR, NH_3-TPD). It also caused a relatively low specific catalytic activity of HPW/Al_2O_3 and HPW/alumina-grafted silicas covered with a bulk-like alumina layer in the three selected testing reactions (Table 3). Fig. 12 illustrates the amounts of HPW adsorbed per square meter of support on all of the alumina-grafted silica materials used (which corresponds to the HPW surface capacity of alumina-grafted materials) versus the aluminum surface concentration ($\mu mol_{Al}/m^2$) in these supports. For aluminum surface concentrations smaller than 10 $\mu mol_{Al}/m^2$, corresponding to partial and nearly full alumina coverages, the support HPW surface capacity increased proportionally to the alumina content reflected in the constant HPW/Al molar ratio. This could arise from the presence of a distinct amount of sites for anchoring the molecular HPW moieties that possess small alumina clusters present at the silica surface at partial coverage. Increasing the amount of grafted alumina in this partial coverage range enhances the total concentration of these sites but does not change their nature and HPW adsorption mode. Moreover, the linear increase in HPW adsorption capacity with the increase in Al surface concentration on the silica surface and leveling of this capacity at higher Al surface concentrations are consistent with the earlier designation of silica coverage with grafted alumina as partial, monolayer, or multilayer.

Thus, the state of adsorbed HPW moieties at partial and monolayer coverages of a silica surface with alumina remains unchanged and maintains constant specific acidity and TOF in MTBE synthesis. However, it is lower than for homogeneous pure HPW for IP dehydration and *t*-butylation of catechol (Table 3). The change in overall charge caused by the interaction of protons with the support and their consequent localization could be a source for the apparently lower specific catalytic activity of adsorbed HPW relative to bulk HPW.

The possible adsorption mechanism of HPW for this case is illustrated in Fig. 13, left. It includes dehydroxylation of surface alumina atoms, Al(OH)–O–Al(OH) → $Al^{(+)}$–O–Al–$O^{(-)}$ + H_2O, which creates a pair of basic (electron-donating, Al–$O^{(-)}$) and acidic (electron acceptor,

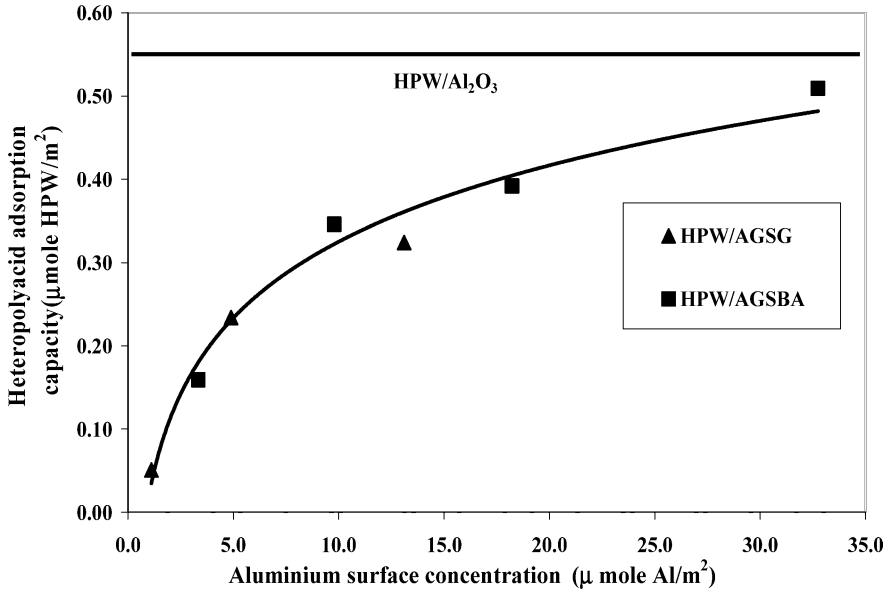

Fig. 12. Effect of aluminum surface concentration in alumina-grafted silica-gel and SBA-15 on $H_3PW_{12}O_{40}$ adsorption capacity of corresponding silicas.

$Al^{(+)}$) sites [23,61,62]. They probably play the role of anchoring sites at the support surface according to the chelate adsorption mechanism. Binding of delocalized protons at the surface of HPW polyanions by interaction with surface basic site creates an excess negative charge (δ^-) at the Keggin unit that causes its additional electrostatic binding by the Lewis acid site. It yields a monodentate (using only one proton) chelation of polyanions. The supposed bonding mode of polyanions also explains the distortion of their structure (^{31}P MAS NMR) compared with that of the bulk heteropolyacid.

In the model proposed for the immobilization of HPW on an alumina-grafted silica surface, HPW is anchored to the support surface via one of the protons compensating for the negative charge of the heteropolyacid polyanion. It allows at least two of the remaining protons to remain delocalized and interact with the reactant molecules in catalytic cycles. This should lead to a decrease in the number of active acidic protons per adsorbed Keggin unit relative to that in the pure HPW that must be reflected by a decrease in measured TOF. Such a decrease was observed in IP dehydration and catechol alkylation with *t*-butanol (Table 3). The fact that the TOFs in MTBE synthesis measured with HPW adsorbed to alumina-grafted silicas were comparable to that measured with the pure HPW can be evidence of good accessibility to reacting molecules of "binding" protons that retain acidic properties. These "binding" protons exhibit lower acidic strength relative to the free protons of the pure HPW acid due to a decrease in mobility, as found from NMR data. But in reactions catalyzed by weak acid sites, such as MTBE synthesis [63], the TOFs measured with HPW supported on alumina-grafted silicas are comparable to that measured with the bulk HPW. In the case of HPW supported on bulk alumina, binding of Keggins by two or even three protons to the support surface should decrease the strength of acidic sites relative to HPW anchored to alumina-grafted silicas because of lower proton mobility and shielding of the proton charge by the high-density basic surface oxygens of the support. It also can cause steric hindrance for the interaction of weakly acidic "binding" protons with reacting molecules, decreasing the effective concentration of acid sites. This is reflected in the NH_3-TPD data (Fig. 11) and is consistent with the distortion of adsorbed Keggin units observed by FTIR and NMR methods. Hence the TOFs measured for all three reactions with HPW/Al_2O_3 catalyst were the lowest The line intensities in the downfield band in HPW/Al_2O_3 ^{31}P MAS NMR spectra (Fig. 10) show a possible increase in the crystal sizes of HPW, which in turn can be correlated with the lowering of the catalytic activity of this sample (Fig. 2).

Formation of a bulk-like alumina phase at the surface of silica supports after multistep alumina grafting decreases the amount of adsorbed HPW per micromole of added aluminum, making it close to that measured on pure Al_2O_3 (Fig. 12). This at least partially reflects the higher number of surface basic sites involved in the immobilization of HPW species per Keggin unit. It could cause a bi- and even tridentate adsorption of molecular HPW moieties by a chelating mechanism as shown in Fig. 13, right, through the use of two or even all three strongly acidic protons belonging to HPW polyanions. An order of magnitude higher density of basic sites at the surface of bulk alumina phase relative to alumina-grafted silicas below and up to their full coverage with alumina changes the HPW adsorption mode as shown in Fig. 13. It decreased the catalyst activity of HPW immobilized on the silica supports covered with alumina multilayers in all of the testing reactions (Fig. 2), for the same reason as on the surface of pure alumina.

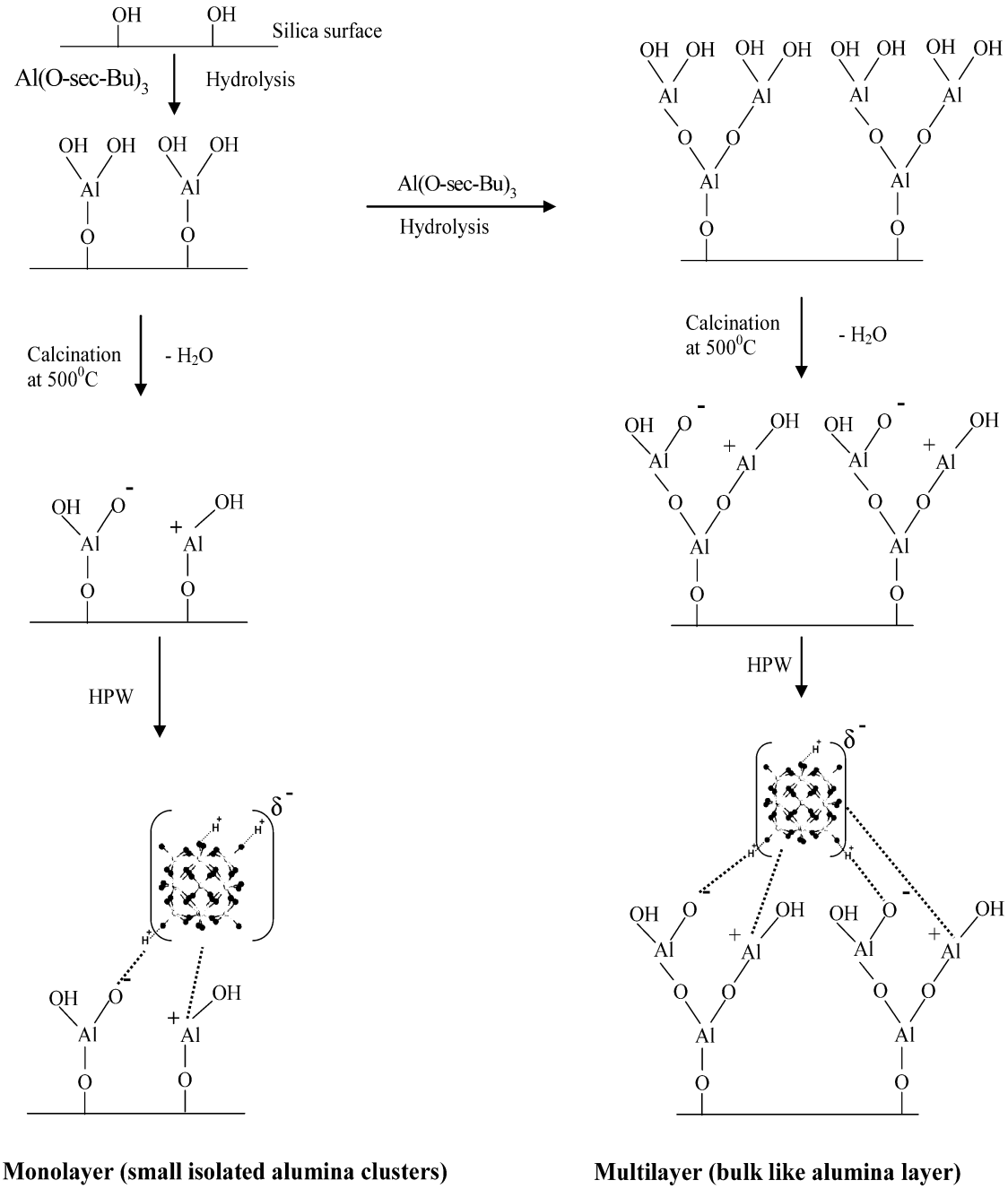

Fig. 13. Models of $H_3PW_{12}O_{40}$ adsorption at the surface of alumina-grafted silica at partial and upto full surface coverage with alumina (left) and at the surface of alumina phase (right).

4. Conclusions

The strong polydentate adsorption of molecular HPW species that retain their structure at the pure alumina surface causes low catalytic activity in acid-catalyzed reactions. It seems that the adsorption of HPW proceeds by a chelating mechanism that involves interactions between acidic protons—Keggin polyanions and the pairs of basic-Lewis acid sites formed at the alumina surface as a result of dehydroxylation. Silica does not adsorb HPW and cannot immobilize it against leaching in polar reaction media. Grafting of silica (regular silica gel or mesostructured SBA-15) with small alumina clusters at partial to full coverage produces isolated basic sites with the same strength as found at the surface of pure alumina, but at a surface concentration that is an order of magnitude lower (site density). It affords a monodentate adsorption of molecular HPW moieties. This causes a strong enough immobilization of HPW at the solid surface to prevent its leaching in polar reactant solutions while retaining its high acidity and catalytic activity in different catalytic reactions. The HPW adsorption capacity per mole of grafted alumina and catalytic activity of

supported HPW materials passes through a maximum with increasing amount of alumina inserted into the silica support by grafting. Using mesostructured SBA-15 as a support yields optimized catalysts with 30–70% higher activity compared with that based on regular silica gel. This is a result of higher surface area and surface concentration of silanols in SBA-15. The latter makes it possible to load more active HPW phase into the optimized catalyst relative to silica gel and to obtain a more active catalytic material.

Acknowledgments

The study was supported by the Israel Science Foundation, Center of Excellence (grant no. 8003). The authors gratefully acknowledge Dr. A. Erenburg for conducting the XRD and Dr. N. Froumin for conducting the XPS experiments.

References

[1] Y. Izumi, K. Urabe, M. Onaka, Zeolite, Clay and Heteropoly Acid in Organic Reactions, VCH, New York, 1992, p. 99.
[2] M. Misono, Chem. Commun. (2001) 1141.
[3] S. Tatematsu, T. Hibi, T. Okuhara, M. Misono, Chem. Lett. (1980) 865.
[4] A. Kukovecz, Z. Balogi, Z. Konya, M. Toba, P. Lentz, S.I. Niwa, F. Mizukami, A. Molnar, J.B. Nagy, I. Kiricsi, Appl. Catal. A 228 (2002) 83.
[5] A. Lapkin, B. Bozkaya, T. Mays, L. Borello, K. Edler, B. Crittenden, Catal. Today 81 (2003) 611.
[6] K.M. Rao, R. Gobetto, A. Ianibello, A. Zecchina, J. Catal. 119 (1989) 512.
[7] L.R. Pizzio, C.V. Caceres, M.N. Blanco, Appl. Catal. A: Gen. 167 (1998) 283.
[8] A. Bielanski, A. Lubanska, J. Pozniczek, A. Micek-Ilnicka, Appl. Catal. A: Gen. 238 (2003) 239.
[9] L.R. Pizzio, P.G. Vazquez, C.V. Caceres, M.N. Blanco, Appl. Catal. A: Gen. 256 (2003) 125.
[10] F. Marme, G. Coudurier, J.C. Vedrine, Micropor. Mesopor. Mater. 22 (1998) 151.
[11] J.F. Knifton, J.C. Edwards, Appl. Catal. A: Gen. 183 (1999) 1.
[12] P. Vazquez, L. Pizzio, G. Romanelli, J. Autino, C. Caceres, M. Blanco, Appl. Catal. A: Gen. 235 (2002) 233.
[13] T. Okuhara, M. Kimura, T. Kawai, Z. Xu, T. Nakato, Catal. Today 45 (1998) 73.
[14] T. Ito, K. Inumaru, M. Misono, Chem. Mater. 13 (2001) 824.
[15] J.G. Hernandez-Cortez, T. Lopez, M.E. Manriquez, R. Gomez, J. Navarrete, J. Sol–Gel Sci. Technol. 26 (2003) 213.
[16] B. Bachiller-Baeza, J.A. Anderson, J. Catal. 212 (2002) 231.
[17] S.R. Mukai, T. Sugiyama, H. Tamon, Appl. Catal. A: Gen. 256 (2003) 99.
[18] W. Kim, M. Kim, J. Kim, G. Seo, Micropor. Mesopor. Mater. 57 (2003) 113.
[19] J. Haber, K. Pamin, L. Matachowski, D. Mucha, Appl. Catal. A: Gen. 256 (2003) 141.
[20] S. Hodjati, K. Vaezzadeh, C. Petit, V. Pitchon, A. Kiennemann, Top. Catal. 16/17 (2001).
[21] S. Soled, S. Miseo, G. McVicker, W.E. Gates, A. Gutierrez-Carrillo, J. Paes, J. Chem. Eng. 64 (1996) 247.
[22] K. Tanabe, M. Misono, Y. Ono, New Solid Acids and Bases. Their Catalytic Properties, Elsevier, Amsterdam, 1989, p. 78.
[23] A.L. Blumenfeld, J.J. Fripiat, Top. Catal. 4 (1997) 119.
[24] P.M. Rao, A. Wolfson, M.V. Landau, M. Herskowitz, Catal. Commun. 5 (2004) 327.
[25] P. Iengo, M.D. Serio, A. Sorrentino, V. Solinas, E. Santacesaria, Appl. Catal. A: Gen. 167 (1998) 85.
[26] M.V. Landau, E. Dafa, M.L. Kaliya, T. Sen, M. Herskowitz, Micropor. Mesopor. Mater. 49 (2001) 65.
[27] A. Goldbourt, M.V. Landau, S. Vega, J. Phys. Chem. B 107 (2003) 724.
[28] D. Zhao, J. Sun, Q. Li, G.D. Stucky, Chem. Mater. 12 (2000) 275.
[29] S. Evans, Surf. Interface Anal. 17 (1991) 85.
[30] G.D. Yadav, N.S. Asthana, V.S. Kamble, J. Catal. 217 (2003) 88.
[31] R.T. Sanderson, Inorganic Chemistry, Rheinhold, New York, 1976.
[32] R.T. Sanderson, Chemical Bonds and Bond Energy, Academic Press, New York, 1976.
[33] W.J. Mortier, Struct. Bonding 66 (1987) 125.
[34] M. Huang, S. Kaliaguine, J. Chem. Soc. Faraday Trans. 88 (1992) 1327.
[35] J.S. Valente, F. Figueras, M. Gravelle, P. Kumbhar, J. Lopez, J.-P. Besse, J. Catal. 189 (2000) 370.
[36] C. Sun, J.C. Berg, Adv. Colloid Interface Sci. 105 (2003) 151.
[37] S. Damyanova, L. Dimitrov, R. Mariscal, J.L.G. Fierro, L. Pertov, L. Sobrados, Appl. Catal. A: Gen. 256 (2003) 183.
[38] L.D. White, C.P. Tripp, J. Colloid Interface Sci. 232 (2000) 400.
[39] B.L. Newalkar, J. Olanrewaju, S. Komarneni, Chem. Mater. 13 (2001) 552.
[40] B.-G. Park, W. Guo, X. Cui, J. Park, C.-S. Ha, Micropor. Mesopor. Mater. 66 (2003) 229.
[41] J.M. Saniger, Mater. Lett. 22 (1995) 109.
[42] L.L. Prado, P.A.P. Nascente, S.C.D. Castro, Y. Gushikem, J. Mater. Sci. 35 (2000) 449.
[43] A. Ghanbari-Siahkali, A. Philippou, J. Dwyer, M.W. Anderson, Appl. Catal. A: Gen. 192 (2000) 57–69.
[44] N. Essayem, A. Holmqvist, P.Y. Gayraud, J.C. Vedrine, Y. Ben Taarit, J. Catal. 197 (2001) 273–280.
[45] P.A. Jalil, M.A. Al-Daous, A.A. Al-Arfaj, A.M. Al-Amer, J. Beltramini, S.A.I. Barri, Appl. Catal. A: Gen. 207 (2001) 159.
[46] W. Kuang, A. Rives, M. Fournier, R. Hubaut, Appl. Catal. A: Gen. 250 (2003) 221.
[47] J.A. Dias, E. Caliman, S.C.L. Dias, M. Paulo, A.T.C.P. de Souza, Catal. Today 85 (2003) 39–48.
[48] E. Lopez-Salinas, J.G. Hernandez-Cortez, I. Schifter, E. Torres-Garcia, J. Navarrete, A. Gutierrez-Carrillo, T. Lopez, P.P. Lottici, D. Bersani, Appl. Catal. A: Gen. 193 (2000) 215.
[49] I.V. Kozhevnikov, K.R. Kloetstra, A. Sinnema, H.W. Zandbergen, H.V. Bekkum, J. Mol. Catal. A: Chem. 114 (1996) 287.
[50] J.C. Edwards, C.Y. Thiel, B. Benac, J.F. Knifton, Catal. Lett. 51 (1998) 77.
[51] H. Pfeifer, D. Freude, M. Hunger, Zeolites 5 (1985) 274.
[52] T. Baba, Y. Hasada, M. Nomura, Y.-I. Ohno, Y. Ono, J. Mol. Catal. A: Chem. 114 (1996) 247.
[53] T. Baba, Y. Ono, Appl. Catal. A: Gen. 181 (1999) 227.
[54] I.V. Kozhevnikov, M.N. Timofeeva, J. Mol. Catal. 75 (1992) 179.
[55] V.M. Mastikhin, V.V. Terskikh, M.N. Timofeeva, O.P. Krivoruchko, J. Mol. Catal. A: Chem. 95 (1995) 135–140.
[56] B. Pawelec, S. Damyanova, R. Mariscal, J.L.G. Fierro, J. Catal. 223 (2004) 86.
[57] N. Essayem, Y.Y. Tong, H. Jobic, J.C. Vedrine, Appl. Catal. A: Gen. 194–195 (2000) 109.
[58] S. Uchida, K. Inumaru, M. Misono, J. Phys. Chem. B 104 (2000) 8108.
[59] M.E. Chimienti, L.R. Pizzio, C.V. Caceres, M.N. Blanco, Appl. Catal. A: Gen. 208 (2001) 7.
[60] V.M. Mastikhin, S.M. Kulikov, A.V. Nosov, I.V. Kozhevnikov, I.L. Mudrakovsky, M.N. Timofeeva, J. Mol. Catal. 60 (1990) 65.
[61] K. Tanabe, M. Misono, Y. Ono, H. Hattori, Stud. Surf. Sci. Catal. 51 (1989) 78.
[62] J.J. Fitzgerald, Solid State NMR Spectroscopy of Inorganic Materials, ACS Symp. Ser., 1999, p. 717.
[63] K.H. Chang, J. Geon, W.S. Ahn, Ind. Eng. Chem. Res. 31 (1992) 125.